

Christian Gerecke | Alexander Edlich | Michael Giubudagian  
Fabian Schumacher | Nan Zhang | Andre Said | Guy Yealland  
Silke B. Lohan | Falko Neumann | Martina C. Meinke | Nan Ma  
Marcelo Calderón | Sarah Hedtrich | Monika Schäfer-Korting  
Burkhard Kleuser

## Biocompatibility and characterization of polyglycerol-based thermoresponsive nanogels designed as novel drug-delivery systems and their intracellular localization in keratinocytes

Suggested citation referring to the original publication:  
Nanotoxicology 11:2 (2017), pp. 267–277  
DOI <http://dx.doi.org/10.1080/17435390.2017.1292371>  
ISSN (print) 1743-5390  
ISSN (online) 1743-5404

Postprint archived at the Institutional Repository of the Potsdam University in:  
Postprints der Universität Potsdam  
Mathematisch-Naturwissenschaftliche Reihe ; 335  
ISSN 1866-8372  
<http://nbn-resolving.de/urn:nbn:de:kobv:517-opus4-395325>



## Biocompatibility and characterization of polyglycerol-based thermoresponsive nanogels designed as novel drug-delivery systems and their intracellular localization in keratinocytes

Christian Gerecke<sup>a</sup>, Alexander Edlich<sup>a</sup>, Michael Giulbudagian<sup>b</sup>, Fabian Schumacher<sup>a,c</sup>, Nan Zhang<sup>d</sup>, Andre Said<sup>d</sup>, Guy Yealland<sup>d</sup>, Silke B. Lohan<sup>e</sup>, Falko Neumann<sup>b</sup>, Martina C. Meinke<sup>e</sup>, Nan Ma<sup>f</sup>, Marcelo Calderón<sup>b</sup>, Sarah Hedtrich<sup>d</sup>, Monika Schäfer-Korting<sup>d</sup> and Burkhard Kleuser<sup>a</sup>

<sup>a</sup>Institute of Nutritional Science, Department of Nutritional Toxicology, University of Potsdam, Arthur-Scheunert-Allee 114-116, Nuthetal, Germany; <sup>b</sup>Institute of Chemistry and Biochemistry, Freie Universität Berlin, Berlin, Germany; <sup>c</sup>Department of Molecular Biology, University of Duisburg-Essen, Essen, Germany; <sup>d</sup>Institute for Pharmacy (Pharmacology and Toxicology), Freie Universität Berlin, Berlin, Germany; <sup>e</sup>Charité – Universitätsmedizin Berlin, Department of Dermatology, Venerology and Allergology, Center of Experimental and Applied Cutaneous Physiology, Berlin, Germany; <sup>f</sup>Institute of Biomaterial Science and Berlin-Brandenburg Center for Regenerative Therapies, Helmholtz-Zentrum Geesthacht, Teltow, Germany

### ABSTRACT

Novel nanogels that possess the capacity to change their physico-chemical properties in response to external stimuli are promising drug-delivery candidates for the treatment of severe skin diseases. As thermoresponsive nanogels (tNGs) are capable of enhancing penetration through biological barriers such as the *stratum corneum* and are taken up by keratinocytes of human skin, potential adverse consequences of their exposure must be elucidated. In this study, tNGs were synthesized from dendritic polyglycerol (dPG) and two thermoresponsive polymers. tNG\_dPG\_tPG are the combination of dPG with poly(glycidyl methyl ether-co-ethyl glycidyl ether) (p(GME-co-EGE)) and tNG\_dPG\_pNIPAM the one with poly(N-isopropylacrylamide) (pNIPAM). Both thermoresponsive nanogels are able to incorporate high amounts of dexamethasone and tacrolimus, drugs used in the treatment of severe skin diseases. Cellular uptake, intracellular localization and the toxicological properties of the tNGs were comprehensively characterized in primary normal human keratinocytes (NHK) and in spontaneously transformed aneuploid immortal keratinocyte cell line from adult human skin (HaCaT). Laser scanning confocal microscopy revealed fluorescently labeled tNGs entered into the cells and localized predominantly within lysosomal compartments. MTT assay, comet assay and carboxy-H2DCFDA assay, demonstrated neither cytotoxic or genotoxic effects, nor any induction of reactive oxygen species of the tNGs in keratinocytes. In addition, both tNGs were devoid of eye irritation potential as shown by bovine corneal opacity and permeability (BCOP) test and red blood cell (RBC) hemolysis assay. Therefore, our study provides evidence that tNGs are locally well tolerated and underlines their potential for cutaneous drug delivery.

### ARTICLE HISTORY

Received 21 December 2016  
Revised 3 February 2017  
Accepted 3 February 2017



### KEYWORDS


Drug delivery;  
nanoparticles; particle  
characterization; keratino-  
cytes; nanotoxicology

### Introduction

Nanocarriers are increasingly important drug-delivery systems for the topical therapy of skin diseases (Zhang et al., 2013). They offer several desirable features, including enhancement of the solubility and stability of highly hydrophobic drugs and improved stability of labile agents, an ability to target encapsulated or incorporated drugs to specific cell types and controlled release. Of major interest for topical drug delivery are polymeric nanoparticles, nano-emulsions, lipid-based nanoparticles and dendrimers. Dendrimers composed of dendritic polyglycerol (dPG) are hyperbranched synthetic macromolecules that exhibit high-water solubility and biocompatibility (Goyal et al., 2016; Witting et al., 2015; Yang et al., 2012). Interestingly, dPG can serve as a macromolecular reagent to fabricate cross-linked hydrophilic three-dimensional polymeric networks referred to as nanogels (Asadian-Birjand et al., 2012a, 2015; Kabanov & Vinogradov, 2009). Moreover, dPG-based

nanogels that respond to external stimuli such as temperature may enable targeted and controlled drug transport (Bergueiro & Calderon, 2015; Cuggino et al., 2011a). In particular, thermoresponsive dPG-based nanogels (tNGs) are NGs fabricated of dPG cross-linked by thermoresponsive polymers such as poly(N-isopropylacrylamide) (pNIPAM) or poly(glycidyl methyl ether-co-ethyl glycidyl ether) (p(GME-co-EGE)), a linear polyglycerol derivate (tPG) (Cuggino et al., 2011b; Giulbudagian et al., 2014). These tNGs undergo a reversible phase-transition at the cloud point temperature ( $T_{cp}$ ) of the polymer. They can be loaded with water-soluble or amphiphilic drugs, as well as biomacromolecules such as proteins, and have been shown to significantly increase drug penetration depth even of large molecules compared to conventional formulations (Witting et al., 2015). However, the loading content of dPG-based tNGs with highly hydrophobic drugs (e.g. potent glucocorticoids, tacrolimus) for the treatment of severe inflammatory skin diseases, to the best of our knowledge, has not been

**CONTACT** Burkhard Kleuser  [kleuser@uni-potsdam.de](mailto:kleuser@uni-potsdam.de)  Institute of Nutritional Science (Department of Toxicology), University of Potsdam, Arthur-Scheunert-Allee 114-116, 14558 Nuthetal, Germany

 Supplemental data for this article can be accessed here.

© 2017 The Author(s). Published by Informa UK Limited, trading as Taylor & Francis Group

This is an Open Access article distributed under the terms of the Creative Commons Attribution-NonCommercial-NoDerivatives License (<http://creativecommons.org/licenses/by-nc-nd/4.0/>), which permits non-commercial re-use, distribution, and reproduction in any medium, provided the original work is properly cited, and is not altered, transformed, or built upon in any way.

investigated. Moreover, dPG-based tNGs are capable of enhancing penetration through biological barriers such as the *stratum corneum* of human skin, penetrate into the hair follicles and can be taken up by cells (Rancan et al., 2016; Sahle et al., 2017; Samah et al., 2010). Therefore, it is of utmost importance to conduct a detailed toxicological evaluation, since there are only a few studies on the adverse biological effects of tNGs in skin cells, especially keratinocytes (Naha et al., 2010).

In the current study, the loading content of the antipsoriatic and anti-inflammatory drugs dexamethasone (DX) and tacrolimus (TAC) in tNGs was determined by isotope-dilution liquid chromatography tandem-mass spectrometry (LC-MS/MS). As there is a growing interest in dermal application of nanoparticle-based formulations, primary human keratinocytes and the spontaneously transformed aneuploid immortal keratinocyte cell line from adult human skin (HaCaT) were employed. In order to comprehensively characterize the toxicological properties of dPG-based tNGs, we analyzed cytotoxic effects by MTT assay, genotoxicity by comet assay and the possible induction of reactive oxygen species (ROS) by a carboxy-H2DCFDA assay. The uptake and intracellular localization of dPG-based tNGs in keratinocytes was imaged by confocal microscopy. In addition, the eye irritation potential of dPG-based tNGs was determined by bovine corneal opacity and permeability (BCOP) test and red blood cell (RBC) hemolysis assay. Here, we are able to highlight the biocompatibility of dPG-based tNGs and underline their potential as a candidate for dermal drug delivery.

## Materials and methods

### Production and characterization of nanogels

Commercially available chemicals from standardized sources were used as delivered. Solvents were purchased as reagent grade and distilled if necessary. Anhydrous solvents were either purchased as ultra-dry solvent (Acros Organics<sup>®</sup>, Geel, Belgium) or received from solvent purification system. For the tPG polymerization reactions, dry toluene was obtained from MBRAUN SPS 800 solvent purification system (Garching, Germany). Water was purified by Millipore water purification system. dPG with average  $M_w$  of 10 kDa (PDI = 1.27) was purchased from Nanopartica GmbH (Berlin, Germany). The amine functionalization of dPG was performed by a previously reported protocol (Fischer et al., 2010) while the degrees of functionalization for dPG-Ac<sub>10%</sub> and dPG-BCN<sub>8%</sub> are given as the percentage of the total hydroxyl groups of the dPG (~135 hydroxyl groups for 10 kDa dPG). Glycidyl methyl ether (GME) (85%) and ethyl glycidyl ether (EGE) (98%; both TCI Europe, Eschborn, Germany) were dried over CaH<sub>2</sub>, distilled and stored over molecular sieves (5 Å). The crosslinking reagent (1R,8S,9S)-bicyclo[6.1.0]non-4-yn-9-ylmethyl (4-nitrophenyl) carbonate was purchased from Synaffix (AE Oss, Netherlands) (Dommerholt et al., 2010). The cyanine dye Indodicarbocyanine (IDCC) was purchased from mivenion GmbH (Berlin, Germany). The synthesis of linear thermoresponsive polymers was performed according to a slightly modified procedure as already reported (Gervais et al., 2010).

The tNGs were synthesized and characterized in accordance to previously reported methods and protocols (Asadian-Birjand et al., 2012b; Cuggino et al., 2011a; Giubudagian et al., 2014). Briefly, for the synthesis of pNIPAM-based nanogels (tNG\_dPG\_pNIPAM), pNIPAM (66 mg), acrylated dendritic polyglycerol (dPG-Ac<sub>10%</sub>) (33 mg), sodium dodecyl sulfate (SDS) (1.8 mg) and ammonium persulfate (APS) (2.8 mg) were dissolved in 5 mL of distilled water. For the fluorescent dye labeled nanogels DCC labeled dPG-Ac<sub>10%</sub> (3 mg) was allowed to react with the unlabeled crosslinker. Argon was bubbled into the reaction mixture for 15 min, which was followed

by stirring under argon atmosphere for another 15 min. The reaction mixture was transferred into a hot bath at 68 °C and polymerization was activated after 5 min with the addition of a catalytic amount of N,N,N',N'-tetramethylethane-1,2-diamine (TEMED; 120 µL). The mixture was stirred at 500 rpm for at least 4 h. For the synthesis of tPG-based nanogels (tNG\_dPG\_tPG), dPG functionalized with (1R,8S,9S)-bicyclo[6.1.0]non-4-yn-9-ylmethyl carbonate (dPG-BCN<sub>8%</sub>) (10 mg) and di-azide functionalized tPG (tPG-(N<sub>3</sub>)<sub>2</sub>) (20 mg) were mixed in 1 mL of dimethylformamide (DMF), cooled in an ice bath and injected with a syringe into 20 mL of water at 45 °C. The mixture was stirred for 3 h and the unreacted alkynes were quenched with azido-propanol or alternatively with IDCC-N<sub>3</sub>.

The tNGs products were purified by dialysis (molecular weight cutoff of the membrane 50 kDa) in water for at least two days. tNG\_dPG\_pNIPAM was then lyophilized to yield the tNGs as a white solid, whereas tNG\_dPG\_tPG was stored as a highly concentrated solution. In addition, the IDCC-labeled nanogels were purified by a Sephadex G25 fine column (GE Healthcare Berlin, Germany), the absence of a free dye was verified by thin-layer chromatography (TLC) (Merck aluminum sheets with silica (corn size 60) and fluorescence marker F254). In total, three batches were produced and characterized independently. tNGs were characterized by <sup>1</sup>H-NMR, dynamic light scattering (DLS) and UV-Vis spectroscopy. The cloud point temperature ( $T_{cp}$ ) was determined by temperature-dependent UV-Vis transmittance measurements.

### Dynamic light scattering (DLS) and zeta ( $\zeta$ ) potential

Size, size distribution and  $\zeta$  potential of tNGs in aqueous or phosphate-buffer solutions were measured at various temperatures by dynamic light scattering using a Zetasizer Nano-ZS 90 (Malvern, UK) equipped with a He-Ne laser ( $\lambda = 633$  nm) under scattering of 173°. For equilibration, all the samples were maintained at the designed temperature for 5 min before testing. Particle sizes and size distribution are given as the average of three measurements. As the DLS measurements of the nanogels had a monomodal distribution and a single exponential decay, the hydrodynamic diameters are reported from the intensity distribution curves.

### Cloud point temperature determination by UV-visible measurement

The  $T_{cp}$  were measured on a Lambda 950 UV/Vis/NIR spectrometer, Perkin Elmer (Rodgau, Germany) equipped with a temperature-controlled, six-position sample holder. PBS buffered (pH 7.4) nanogels solutions were heated at 0.2 °C/min while monitoring both the transmission at 500 nm (1 cm path length) and the solution temperature (from 20 to 60 °C), as determined by the internal temperature probe. The  $T_{cp}$  of each nanogel was defined as the temperature at the inflection point of the normalized transmission curves.

### Compound loading

For loading of DX and TAC, lyophilized pNIPAM-based nanogels (10 mg) and highly concentrated tPG-based nanogels (10 mg) were added to a suspension of tacrolimus (TAC) and dexamethasone (DX) (5 mg) in 2 mL of MilliQ water. The nanogels were let to swell, followed by sonication in a water bath for 30 min. The suspension was stirred overnight at 25 °C and the encapsulated fraction was separated from the free drug by filtration with a 0.45 µm regenerated cellulose syringe filter. Following, 100 µL of the encapsulated fraction were lyophilized for the determination of the total concentration. The drug-loaded nanogels were stored at 4 °C.

### Determination of dexamethasone and tacrolimus loading of nanogels by isotope-dilution LC-MS/MS

Drug-loaded nanogels (polymer concentration: 5 mg/mL) were diluted with water (DX-loaded: 1:500, TAC-loaded: 1:100). Aliquots of these dilutions were mixed with equal volumes of the accordant stable-isotope labeled internal standard, ethanolic 1  $\mu$ M DX- $d_4$  (C/D/N Isotopes, Quebec, Canada) or methanolic 10  $\mu$ M [ $^{13}\text{C}_1$ ,  $d_4$ ]TAC (Alsachim, Illkirch Graffenstaden, France), respectively. Saturated aqueous solutions of DX and TAC were prepared and filtrated using a 0.22  $\mu$ m syringe filter (Carl Roth, Karlsruhe, Germany). The filtrates were centrifuged (16,000  $g$  for 10 min), diluted 1:100 with water and mixed with equal volumes of the appropriate internal standard. All analyses were conducted with an Agilent 1260 Infinity LC system coupled to an Agilent 6490 triple quadrupole-mass spectrometer (Agilent, Waldbronn, Germany) interfaced with an electrospray ion source operating in the positive ion mode (ESI+). Chromatographic conditions and settings of the MS/MS detector for quantification of DX have been published recently (Döge et al., 2016). Chromatographic separation of TAC containing samples was carried out using an Agilent Poroshell 120 EC-C18 column (2.7  $\mu$ m, 3.0  $\times$  50 mm). Aqueous ammonium formate (20 mM, pH 3.5) and methanol (VWR, Darmstadt, Germany) were used as eluents A and B, respectively. Samples (1  $\mu$ L) were injected into a mobile phase consisting of 90% eluent A. TAC and its internal standard [ $^{13}\text{C}_1$ ,  $d_4$ ]TAC were eluted from the column, which was tempered at 25  $^\circ\text{C}$ , with a 4-min linear gradient to and a subsequent isocratic stage for 5 min at 2:98 (v/v) eluent A/B at a flow rate of 0.4 mL/min. TAC and [ $^{13}\text{C}_1$ ,  $d_4$ ]TAC co-eluted from the separation column at 5.6 min. The total run time for one analysis was 13 min, including re-equilibration of the LC system. The ion source parameters were taken from Koster et al. (2013), who used a comparable mass spectrometric configuration for detection of four immunosuppressants including TAC. Quantification of TAC in relation to the internal standard [ $^{13}\text{C}_1$ ,  $d_4$ ] TAC was carried out using the multiple reaction monitoring (MRM) approach. Ammonium adducts  $[\text{M} + \text{NH}_4]^+$  were selected as precursor ions. The collision-induced loss of two hydroxyl groups and ammonium from the precursor ion, represented by  $m/z$  821.5  $>$  768.5 for TAC and  $m/z$  826.5  $>$  773.6 for [ $^{13}\text{C}_1$ ,  $d_4$ ]TAC (collision energy for both mass transitions: 20 V), was used for quantification. Two further mass transitions per compound were recorded as *qualifiers*.

### Isolation and cultivation of keratinocytes

HaCaT cells, a spontaneously transformed aneuploid immortal keratinocyte cell line from adult human skin, were cultured as described in the supplementary information S1. Primary human keratinocytes (NHK) were isolated from juvenile foreskins (with ethical consent) and cultivated according to standard protocols (Gysler et al., 1997). The NHK cells were maintained in Keratinocyte Growth Medium (KGM) supplemented with Bullet Kit (Lonza, Cologne, Germany) at 37  $^\circ\text{C}$  in a humidified atmosphere with 5%  $\text{CO}_2$ . The NHK cells used in all experiments did not exceed passage 4 and were seeded and maintained during experiments in KGM.

### Confocal laser scanning microscopy

NHK were seeded into borosilicate glass bottomed, 8-well Nunc<sup>®</sup> Lab-Tek<sup>®</sup> Chamber Slide<sup>™</sup> system (Sigma-Aldrich, Steinheim, Germany). Following 24 h culture, fresh media was applied and 200  $\mu$ g/mL of indocarbocyanine (IDCC) labeled dPG-pNIPAM or dPG-tPG nanogels applied. Following a further 3, 24 or 48 h incubation, cells were washed three times with phosphate-buffered saline (PBS) and incubated with LysoTracker<sup>®</sup> Red (DND-99, Life

Technologies, Germany) as per the manufacturer's instructions. Cells were then washed and fixed with Paraformaldehyde (PFA). 4',6-diamidino-2-phenylindole (DAPI) counter-staining was subsequently performed. Images were taken using a confocal laser scanning microscope (CLSM) (SP8, Leica, Germany) and analyzed using Fiji image analysis software, an ImageJ distribution (Schindelin et al., 2012).

### Principles of toxicological testing

tNG\_dPG\_pNIPAM and tNG\_dPG\_tPG (stock solution each 5 mg/mL) were tested in concentrations of 0.05 and 0.5 mg/mL, respectively, and in at least three independent experiments ( $n = 3$ ). The negative control was the respective solvent (deionized water for the BCOP test) set 100% for analysis. The positive control was selected according to the event of interest, being Silver nanoparticles (NPs) (diameter 40 nm; Sigma-Aldrich, Steinheim Germany) 5  $\mu$ g/mL for ROS induction and comet assay and SDS 0.002% for MTT test, and 100% (v/v) ethanol for the BCOP test.

### MTT assay

The investigation of potential cytotoxic effects of the tNGs was carried out by 3-(4,5-dimethylthiazol-2-yl)-2,5 diphenyltetrazolium bromide (MTT) reduction assay as already described (Kumar et al., 2014). NHK cells were seeded into 96-well plates (TPP, Trasadingen, Switzerland). After 24 h, the tNGs (0.5 and 0.05 mg/mL final concentration) were added and kept for 24 and 48 h, respectively. Subsequently, the cells were incubated with 100  $\mu$ L MTT solution (0.5 mg/mL in PBS) for 4 h. After removing the supernatants, 50  $\mu$ L dimethyl sulfoxide was added to dissolve the formazan salt and its optical density (OD) was measured using a microplate reader (Tecan, Crailsheim, Germany) setting the excitation to 540 nm. The positive controls were treated with 0.002% SDS. A cell viability  $<$ 75% predicts cytotoxic effects.

### Determination of ROS induction

Intracellular ROS levels were measured using the 6-carboxy-2',7'-dichlorodihydrofluorescein diacetate (carboxy-H2DCFDA) assay as described previously (Hönzke et al., 2016). NHK were seeded in 12-well plates (100,000 cells per well) and grown for 24 h (37  $^\circ\text{C}$ , 5%  $\text{CO}_2$ ) in KGM (Lonza, Cologne, Germany). The next day, cells were incubated with tNGs (0.5 and 0.05 mg/mL final concentration) for 0.5 h, 1 h, 2 h, 3 h, 4 h and for 24 h in KGM. After exposure, cells were loaded with 25  $\mu$ M Carboxy-H2DCFDA in KGM for 1 h at 37  $^\circ\text{C}$ . The cells were harvested and cell pellets were washed five times with ice-cold FACS buffer (0.1% sodium azide, 0.5% bovine serum albumin (BSA) in PBS). The samples were analyzed on a FACSCanto II (BD Biosciences, Heidelberg, Germany), which counted 10,000 events. The Carboxy-H2DCFDA fluorophore was measured in the FITC channel (488 nm excitation). Silver NPs (Sigma-Aldrich, Steinheim Germany) (diameter 40 nm) served as positive control. The results are presented as mean  $\pm$  standard error of the mean (SEM) of three independent experiments. All data were normalized to the vehicle control prior to statistical analysis.

### Alkaline single-cell gel electrophoresis (comet assay)

DNA strand breaks, DNA cross-links and alkali labile sites (ALSs) were detected after 24 h of exposure to tNG\_dPG\_tPG and tNG\_dPG\_pNIPAM (0.5 and 0.05 mg/mL final concentration) by the alkaline version (pH  $>$  13) of the comet assay as described

elsewhere (Kumar et al., 2014). Analysis of DNA migration was performed by using a fluorescence microscope DXM1200D (Nikon Europe, Düsseldorf, Germany) and Lucia software (Laboratory Imaging, Prague, Czech Republic). At least 50 cells were scored per sample and the results were expressed as mean percent tail length. Exposure to Ag NPs (40 nm diameter, 5 µg/mL) for 24 h was used as positive control. Experiments were performed at least three individual times.

#### Irritation potential red blood cell test (RBC test)

Irritation potential red blood cell (RBC) test was performed according to INVITTOX N°37 protocol (Pape, 1992). RBC diluted with 10 mM glucose to  $4 \times 10^9$  cells/mL was added to tNGs in PBS (0.5 and 0.05 mg/mL final concentration). De-ionized water served as positive control, PBS as negative control and SDS solutions ranging in concentrations from 0 to 80 ppm as hemolysis reference. The absorbance of the released oxyhemoglobin at 560 nm (WPA Biowave, Biochrom Cambridge, UK) was measured and the relation between effective concentration of 50% hemolysis and protein denaturation was calculated to evaluate acute eye irritancy potential.

#### Bovine corneal opacity and permeability test (BCOP)

BCOP test was performed according to OECD guideline 437 (OECD, 2009). Briefly, the cornea of bovine eyes was isolated and washed in Hanks' Balanced Salt Solution (HBSS with  $\text{Ca}^{2+}$  and  $\text{Mg}^{2+}$ ) mounted in the cornea holders with Minimum Essential

Medium (MEM, without Phenol Red; both from Gibco by Life Technologies™, Carlsbad, CA) and measured for initial opacity after 1 h (Opacitometer Kit, BASF-OP 3.0, Ludwigshafen, Germany). Nanogels (0.5 and 0.05 mg/mL final concentration) were added for a period of 10 min, and final opacity was measured after 4 h. Permeability was determined by adding sodium fluorescein solution (4 mg/mL, Sigma-Aldrich, Steinheim, Germany). Spectrophotometric measurements (WPA Biowave, Biochrom, Cambridge, UK) evaluated at 490 nm were recorded as optical density (OD490). De-ionized water was used as negative control, and 100% (v/v) ethanol (VWR, Darmstadt, Germany) as positive control. The final *in vitro* irritancy score (IVIS) was calculated with the equation:  $\text{IVIS} = \text{mean opacity value} + (15 \times \text{mean permeability OD490 value})$ .

## Results

### Characterization of nanogels

The tNGs utilized in this study were synthesized from dPG serving as a macromolecular crosslinking reagent and two kinds of thermoresponsive polymers: pNIPAM and tPG (Figure 1). pNIPAM was used as a robust polymer that preserves its  $T_{\text{cp}}$  of around 34 °C, owing to a neglectable dependence of the  $T_{\text{cp}}$  on the polymer molecular weight or concentration (Figure 2). The transition temperature of tPG by contrast may be fine-tuned through the ratio of its monomers used during the polymerization reaction. The ratio of 1:1 (m:n, Figure 1) for the synthesis of the tPG yielded tNG with  $T_{\text{cp}}$  of 29 °C (Figure 2). The synthesized nanogels had comparable hydrodynamic radii, as determined by DLS, above and

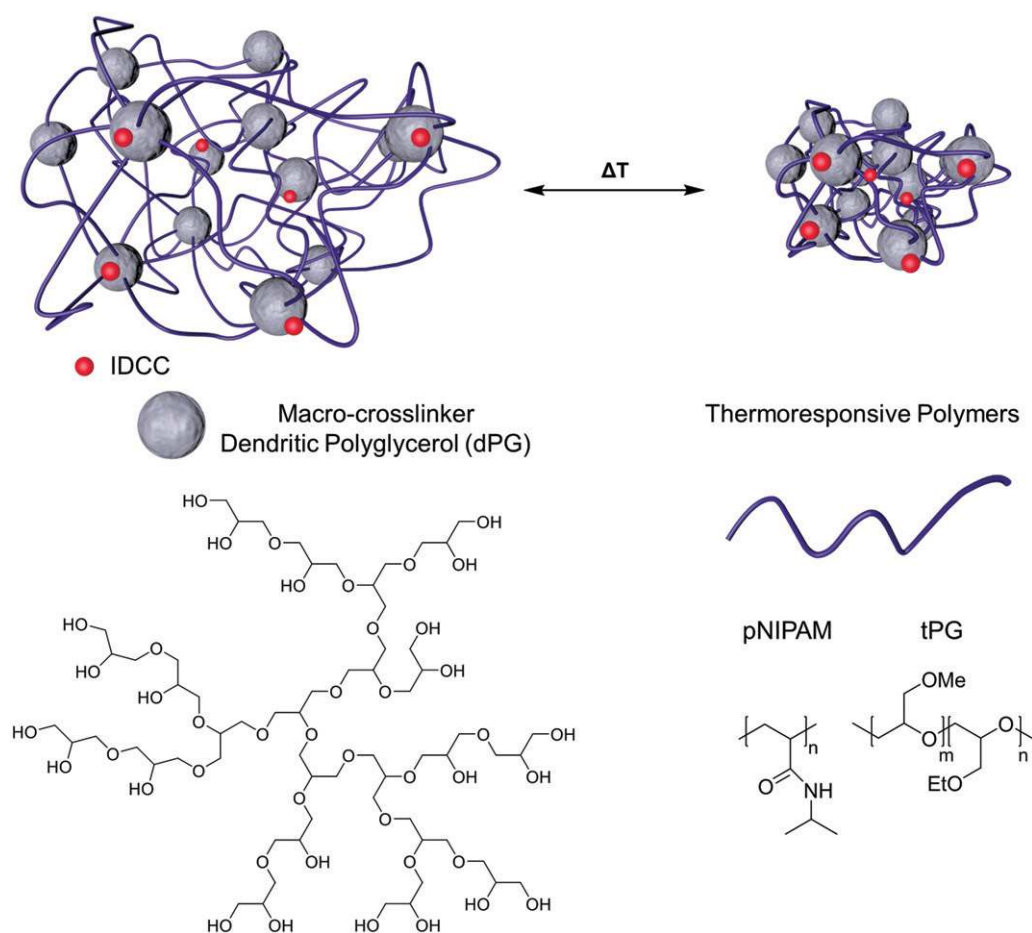
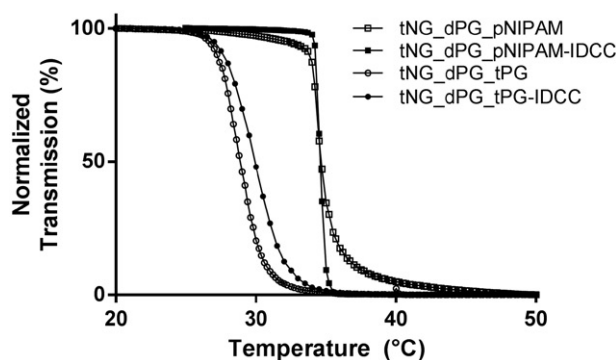


Figure 1. Schematic representation of the tNG and their building blocks.



**Figure 2.** Characterization of tNGs. Normalized transmission of the tNG aqueous solutions as a function of temperature UV-Vis ( $\lambda = 500$  nm).

**Table 1.** The synthesized nanogels and their properties.

Nanogel	Size [nm] (PDI) <sup>a</sup>		$\zeta$ potential [mV] <sup>b</sup>		$T_{cp}$ [°C] <sup>c</sup>
	25 °C	37 °C	25 °C	37 °C	
tNG_dPG_pNIPAM	110.5 (0.194)	87.7 (0.127)	-1.07	-0.447	34.6
tNG_dPG_pNIPAM-IDCC	124.3 (0.297)	91.3 (0.210)	-2.10	-2.13	34.6
tNG_dPG_tPG <sub>(1:1)</sub>	132.9 (0.073)	113.2 (0.067)	0.332	1.14	28.9
tNG_dPG_tPG <sub>(1:1)</sub> -IDCC	157.9 (0.231)	112.3 (0.122)	1.63	3.28	29.8

<sup>a</sup>Size and polydispersity index (PDI) by DLS in water at 25 °C. Measurements were performed in triplicates; intensity average mean value presented.

<sup>b</sup> $\zeta$  potential determined by Zeta-sizer in phosphate buffer. Measurements were performed in triplicates; intensity average mean value presented.

<sup>c</sup>Cloud point temperature determined as the temperature at 50% transmittance by UV-Vis ( $\lambda = 500$ ).

below their  $T_{cp}$  (Table 1). Similarly,  $\zeta$  potential measurements revealed nearly neutral surface charges above and below the  $T_{cp}$ , ranging between  $-2.10$  and  $+3.28$  mV.

### Loading capacity of nanogels with DX and TAC

The tNG-loading capacity of the model drugs DX and TAC was determined by isotope-dilution LC-MS/MS (Figure 3). The low DX concentration in aqueous solution (82.4 mg/L) significantly increases on DX loading in both tNG\_dPG\_tPG (289.3 mg/L) and tNG\_dPG\_pNIPAM (340.0 mg/L). Concordantly, high loading capacities in tNG\_dPG\_tPG (5.8%) and tNG\_dPG\_pNIPAM (6.8%) were detected. As to be expected, TAC was almost insoluble in water (1.22 mg/L). Corresponding to the high loading contents in both tested tNGs (tPG: 2.5% and pNIPAM: 0.9%), tremendous increases of TAC concentrations in solution were measured on tNG loading. Respectively, the tNG\_dPG\_tPG increased the TAC concentration up to 123.9 mg/L and the tNG\_dPG\_pNIPAM up to 44.7 mg/L in solution. In summary, the tNG\_dPG\_tPG increases the solubility of the model drugs DX and TAC in aqueous solution about 3.5-fold and 101.5-fold, respectively. Corresponding values for the tNG\_dPG\_pNIPAM are 4.1-fold and 36.6-fold.

### Imaging the uptake and intracellular localization of tNGs by CLSM

It was of interest to investigate whether the tNGs were recognized and taken up by keratinocytes. For this purpose, the uptake of fluorescently-labeled tNG\_dPG\_tPG-IDCC and tNG\_dPG\_pNIPAM-IDCC into NHK and HaCaT was assessed by confocal microscopy. Following 3 h (Figure S2), 24 h (Figure 4) and 48 h (Figure S3) incubation with tNGs (0.2 mg/mL), intracellular localization was apparent for both tNGs. Lysosomal counter stain revealed strong

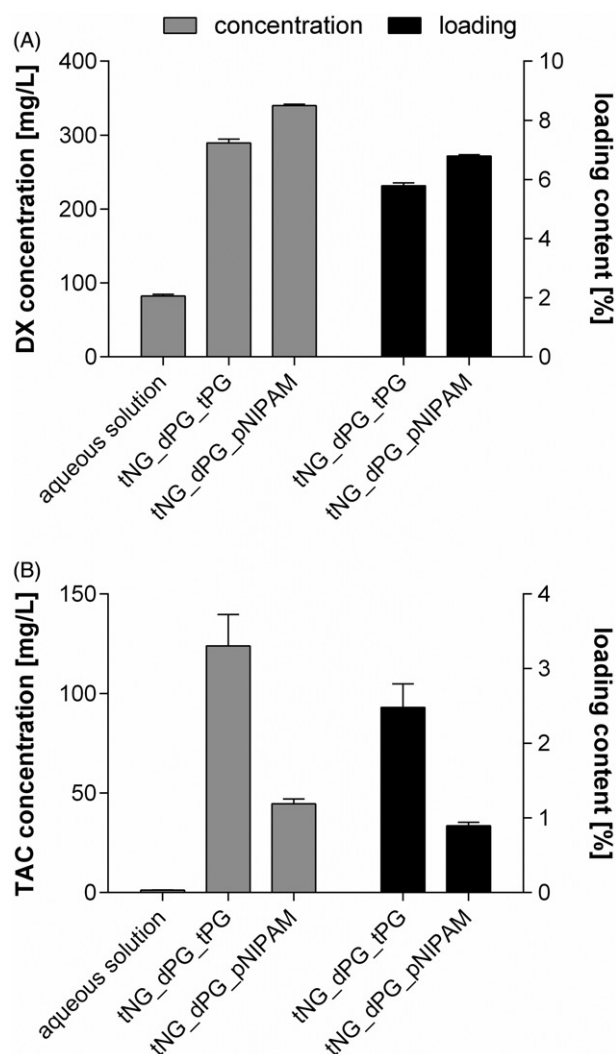


**Figure 3.** (A) DX and (B) TAC loading capacity of studied tNGs as assessed by isotope-dilution LC-MS/MS. Hereby, the drug concentrations in aqueous tNG solutions of defined polymer concentrations (5 mg/mL) as well as the resulting percentage drug loading contents are given. For comparison, concentrations of tNG-free, saturated aqueous drug solutions are presented. Data are means  $\pm$  SEM from three separately prepared tNG batches (each measured thrice) or saturated aqueous drug solutions.

colocalization of the tNGs with lysosomal compartments after 24 h (Figure 4) and 48 h (Figure S3), indicating that the lysosomes are the final or at least a major part of the intracellular fate of the nanogels in NHK cells. These results could be confirmed after 24 h incubation in HaCaT cells (Figure S1).

### Effect of tNGs on keratinocyte cell viability, ROS-production and genotoxicity

MTT viability assays showed no significant induction of cytotoxicity in NHK cells exposed to tNG\_dPG\_tPG and tNG\_dPG\_pNIPAM (0.05 and 0.5 mg/mL, 24 and 48 h incubation) (Figure 5(A,B)). However, no one single toxicity assay can truly encompass the spectrum of mechanisms by which an exogenous agent may harm a cell, owing to distinct biochemical pathways involved and/or subtlety of effect. Nanoparticles have the potential to generate intracellular ROS, one of the most important mechanisms of toxicity related to nanoparticle exposure (Nel et al., 2006). In accordance with other studies, intracellular ROS levels were determined over a 24 h time period at fixed time points by the

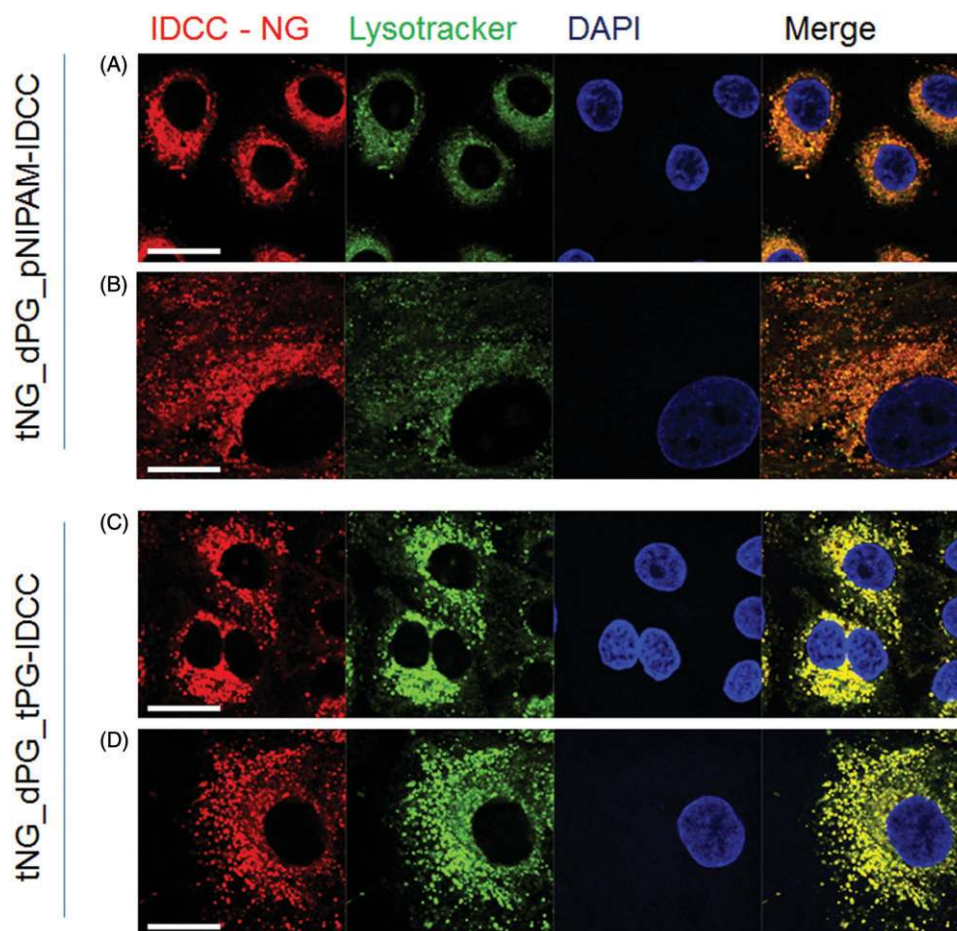


**Figure 4.** Cellular uptake of tNGs by primary keratinocytes. NHK were exposed to 0.2 mg/mL of each tNG for 24 h. Colocalization between tNG\_dPG\_pNIPAM-IDCC (A, B) or tNG\_dPG\_tPG-IDCC (C, D) (IDCC signal pseudo-colored red) and lysosomal compartment (LysoTracker® Red staining, pseudo-colored green) was then assessed by CLSM. Cell nuclei were counterstained with DAPI (pseudo-colored blue). Scale bars represent 25  $\mu$ m.

carboxy-H2DCFDA assay (Mukherjee & Byrne, 2013). However, NHK treated with 0.05 and 0.5 mg/mL tNG\_dPG\_tPG and tNG\_dPG\_pNIPAM over 24 h displayed no increase in their intracellular ROS levels compared to those of control cells (Figure 5(C,D)). The ROS levels were seen to be reduced after 4 h below the untreated control and did not significantly rise above the untreated control values over the 24 h time period. It is well-known that nanoparticles can have genotoxic effects, silver nanoparticles being a key example (Eom & Choi, 2010; Hackenberg et al., 2011). Indeed, the comet assay revealed after incubation of NHK with silver nanoparticles a strong induction of DNA damage. By contrast, no genotoxic effects were observed following exposure to tNG\_dPG\_tPG and tNG\_dPG\_pNIPAM (0.05 and 0.5 mg/mL, 24 h incubation), as the relative tail lengths were not increased (Figure 5(E)). In summary, these results suggest that the tNGs were nontoxic to primary human keratinocytes.

#### Eye irritation potential of tNGs

The BCOP assay and the *in vitro* RBC test were conducted using standardized test protocols to ensure the accuracy, quality and comparability of the obtained results. Here, SDS served as a positive control in the RBC test, inducing 50% hemolysis at 29 ppm. The tNGs showed negligible hemolytic activity at concentrations of 0.05 and 0.5 mg/mL (Figure 6(A)).

For the BCOP assay, an *in vitro* irritation score (IVIS) was calculated to classify the test substance. "Category 1", induction of

serious eye damage is classified as scores  $>55$ , as defined by UN GHS classification system. For scores falling between 3 and 55, "no prediction can be made". Ethanol served as positive control for Category 1, and TiO<sub>2</sub> nanoparticles served as control for slight eye irritation ("No prediction can be made") as previously reported (Hönzke et al., 2016; Warheit et al., 2007). The tNGs, at concentrations of 0.05 and 0.5 mg/mL, revealed IVIS values of less than 3 and thus can be considered as nonirritant to mammalian eyes. In summary, both tNGs were devoid of irritating potential for the eye in our applied biological assays.

#### Discussion

Engineered nanoparticles (NPs) and predominantly inorganic NPs can affect the cell viability as shown in various studies (Ahlberg et al., 2014; Hofmann-Antenbrink et al., 2015). By contrast, polymeric particles can be adjusted to their field of operation and can be loaded for drug delivery (Mak et al., 2012). The tNGs utilized in this study were synthesized from dPG cross-linked by thermoresponsive polymers tPG or pNIPAM (Giulbudagian et al., 2014). The high drug-loading capacity of these tNGs could be shown with the model compounds DX and TAC by isotope-dilution LC-MS/MS in this study. This finding indicates that tNGs are suitable drug-delivery systems by enhancing the water solubility of highly hydrophobic compounds and drugs like TAC. Furthermore, the presented high loading capacities for DX (5.8% in tNG\_dPG\_tPG and 6.8% in tNG\_dPG\_pNIPAM) are comparable to other highly



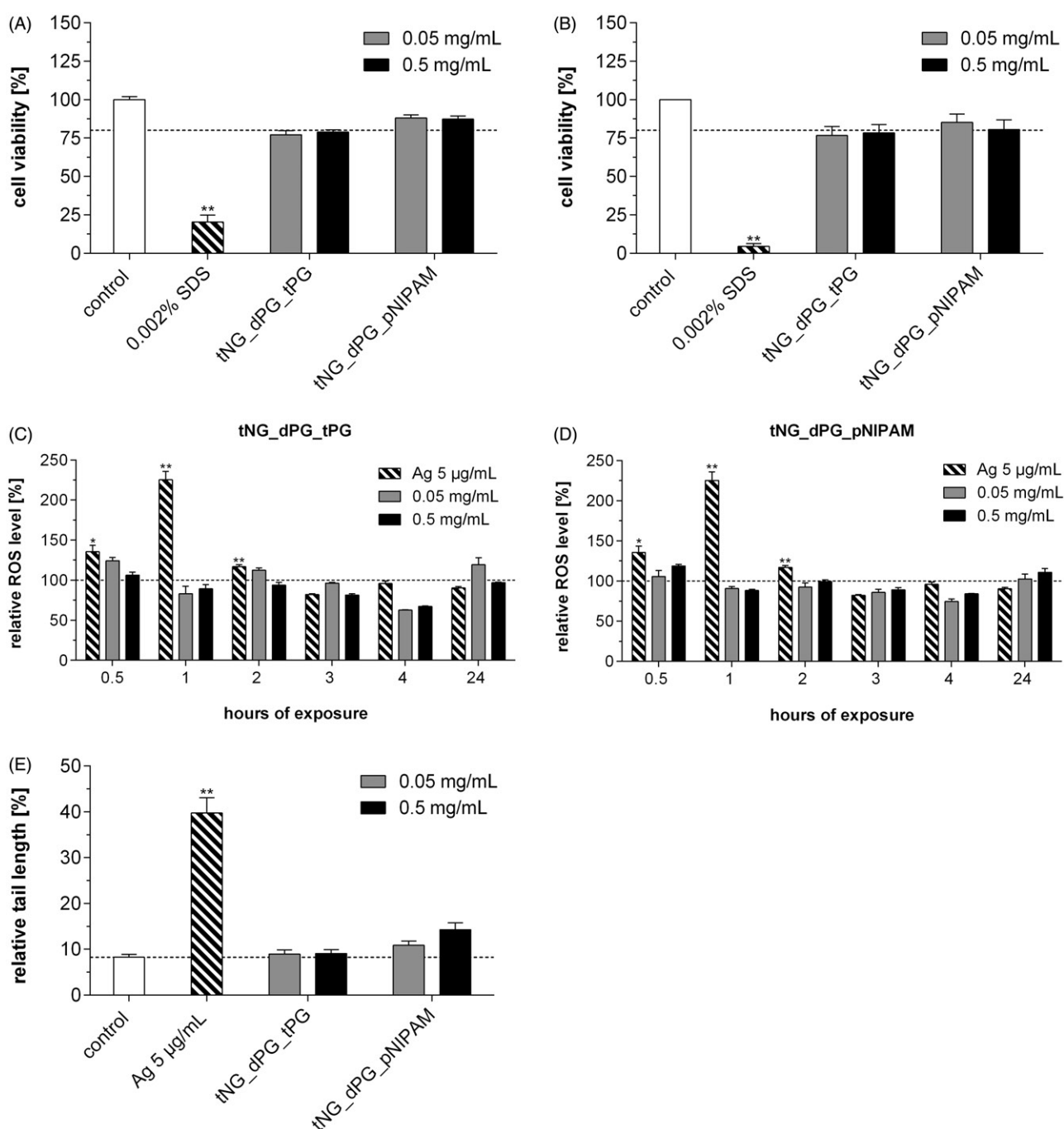


**Figure 5.** Effect of tNGs on cell viability, intracellular ROS and genotoxicity. NHK were exposed to the indicated tNG concentrations for (A) 24 h or (B) 48 h. A declined formazan formation <75% after MTT exposure indicates cytotoxicity. (C, D) ROS were measured via the Carboxy-H2DCFDA assay and FACS analysis. Cells were incubated with the indicated concentrations (0.05 and 0.5 mg/mL) of tNG\_dPG\_tPG (C) and tNG\_dPG\_pNIPAM (D) for a period of 24 h at the indicated time points. Exposure to 5 µg/mL silver nanoparticles served as a positive control. (E) Measurement of DNA damage using the alkaline comet assay. Cells were treated with the indicated tNG concentrations for 24 h. Exposure to 5 µg/mL silver nanoparticles for 24 h served as a positive control. After 24 h, the level of DNA breakage was expressed by the relative tail length. Values are expressed relative to untreated keratinocytes which served for reference (black dotted line). Statistical differences were assessed by one-way ANOVA and Bonferroni's post analyses (mean  $\pm$  SEM;  $n = 3$ ). \*\* $p < 0.01$  indicates a statistically significant difference compared with control cells.

efficient nanocarrier systems (Kim & Martin, 2006; Sun et al., 2015). The TAC loading in tNG\_dPG\_tPG (2.5%) and tNG\_dPG\_pNIPAM (0.9%) was also comparable to other highly efficient nano-based systems (Wang et al., 2016; Xu et al., 2014; Zhao et al., 2015). As the drugs TAC and DX are used for the treatment in skin, it is of high importance that the drugs are being released in the viable epidermis targeting immune cells within the skin. Thermoresponsive tNGs undergo conformational changes at temperatures around their  $T_{cp}$  resulting in water loss and increase of hydrophobicity. In addition, the conformational change at

temperatures close to  $T_{cp}$  changes the loading capacity and leads to a thermal triggered compound release (Rancan et al., 2017; Witting et al., 2015). Since the  $T_{cp}$  of the studied tNGs is close to the physiological skin temperature (32 °C) the described tNGs are capable of releasing their payload into the viable part of the skin, before they are taken up by the non-targeted keratinocytes. This underlines the high importance of the described tNGs as drug carriers, given they are well-tolerated.

As previously described, the tNGs are well-known particles that are capable to deliver loaded drugs or model compounds

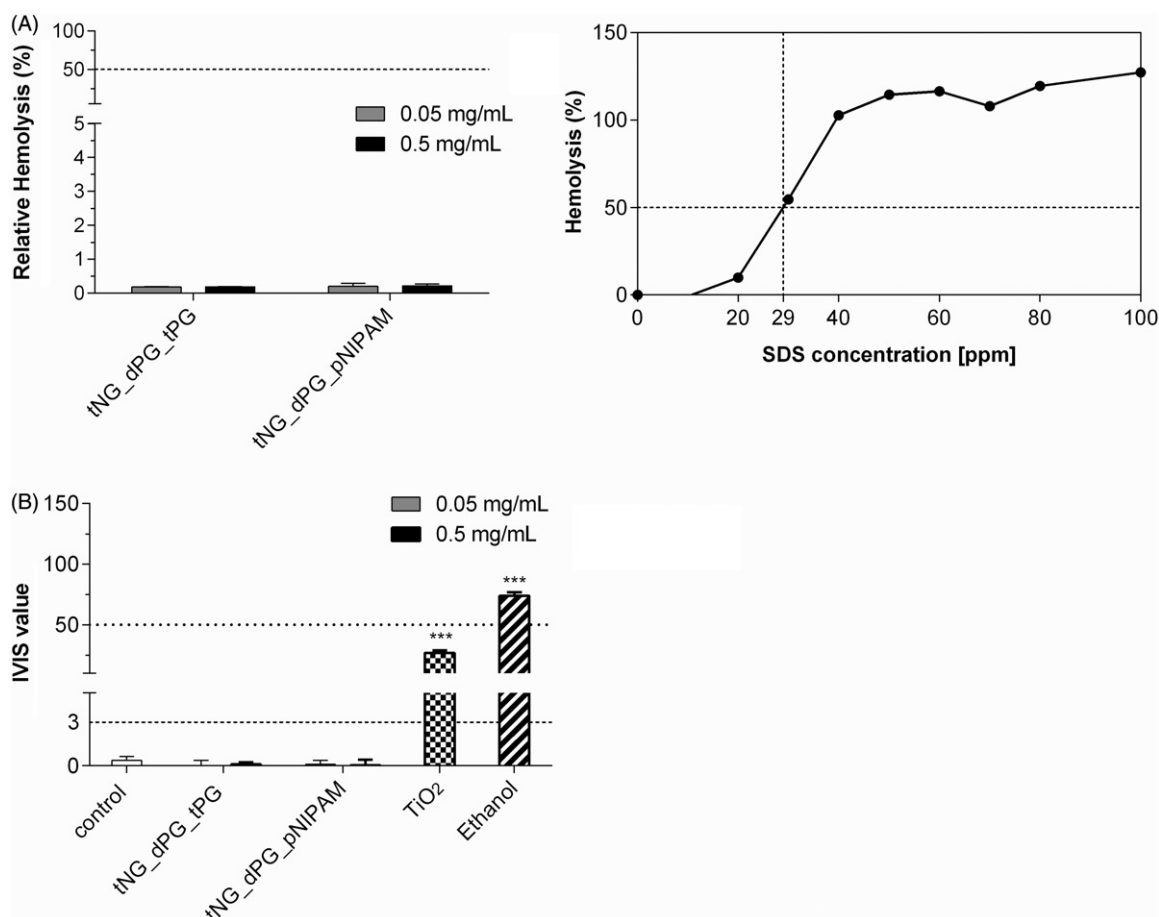


**Figure 6.** Eye irritation potential of tNGs (A) NHK were exposed to the indicated concentrations of tNGs. Then, irritation potential was assessed with RBC test. Negligible hemolysis (%) far under the irritation cutout of 50% by nanogels after 10 min exposure indicates no *in vivo* eye irritation potential. Mean  $\pm$  SEM ( $n=3$ ). (B) Opacity increase and permeability decrease of bovine corneas after incubation with 0.05 and 0.5 mg/mL tNGs as assessed by BCOP test. The final *in vitro* irritancy score (IVIS) is depicted as mean  $\pm$  SEM. ( $n=3$ ). IVIS values are classified into “No Category” ( $\leq 3$ ), as defined by the United Nations Globally Harmonized System of Classification and Labelling of Chemicals (UN GHS). Statistical differences were assessed by one-way ANOVA and Bonferroni’s post analyses.

efficiently into the viable epidermis of human skin which is primarily composed of keratinocytes (Asadian-Birjand et al., 2012a; Samah et al., 2010; Witting et al., 2015). Potential interactions with keratinocytes of the viable epidermis cannot be entirely excluded, particularly in diseased and, hence, barrier impaired skin. As such, assessment of tNG biocompatibility with keratinocytes is of great interest since nanoparticles may interact with various proteins and nucleic structures and could impair cellular functions (Donaldson et al., 2004). In order to identify adverse outcomes, the human immortalized keratinocyte cell line HaCaT and the colon cancer cell line SW480 have been incubated with pNIPAM nanogels in previous studies (Naha et al., 2010). In the present study, the HaCaT cell line and primary keratinocytes were used to determine the biocompatibility of the tNGs.

Firstly, it was necessary to determine whether tNGs can enter keratinocytes. Laser scanning microscopy was used to study the cellular localization of fluorescently labeled tNGs. In accordance with other studies (Rancan et al., 2016), it could be shown that fluorescently labeled tNGs are clearly seen to be internalized by HaCaT and NHK and are predominantly localized within lysosomal compartments (Iversen et al., 2011). Cellular uptake of glucocorticoid and tacrolimus-loaded tNGs will enhance drug access to the cellular target. This should not only hold true for keratinocytes which clearly exceed, e.g. fibroblasts for nanoparticle uptake (Contri et al., 2016), but even the more for dendritic cells. Following this confirmation of tNG internalization, toxicological

assessments were performed. Incubation of NHK with tNGs of either type did not lead to a reduction of the cell viability as assessed by MTT assay. Similarly, the carboxy-H2DCFDA assay revealed no apparent induction of ROS generation following incubation with the tNGs, one of the most important mechanisms of toxicity as a result to nanoparticle exposure (Nel et al., 2006; Petersen & Nelson, 2010). Given the significant impact of potential mutagenesis on a subject’s long-term health, this result is key to the prospective long-term therapeutic use or residence time of nanoparticles (Cooke et al., 2003; Petersen & Nelson, 2010). It has been suggested that the general trend of nanomaterials cytotoxicity is similar among various types of nanoparticles and that non-specific oxidative stress is one of the largest concerns in NP-induced toxicity leading to genotoxicity as well (Nel et al., 2006; Shi et al., 2012). In contrast to ROS measurements, alkaline comet assay experiments detect many types of DNA damage, i.e. strand breaks, alkali labile sites and incomplete excision repair sites (Kumaravel et al., 2009). Well in line with the previous assays, tNGs did not exhibit any genotoxic potential. Therefore, the biocompatibility of the unlabeled tNGs was further confirmed by the genotoxicity results.

By including multiple aspects of cutaneous toxicity assessment, such as cytotoxicity, genotoxicity and ROS induction in NHK, as well as aspects of interactions with skin components such as cell uptake and cellular fate, a detailed evaluation of the prospective local toxicity of tNGs in human skin has been performed.

Furthermore, the potential irritancy of tNGs following unintended contact with the eye was assessed using the BCOP assay and RBC test, the effectiveness of which has recently been demonstrated (Hönzke et al., 2016; Kolle et al., 2016; Kumar et al., 2014). Our results clearly indicate that tNGs are devoid of irritating potential for the eye, irrespective of the individual thermoresponsive polymer used. Direct comparison of the tNGs with TiO<sub>2</sub> as a nanomaterial reference, demonstrates that tNG\_dPG\_tPG and tNG\_dPG\_pNIPAM nanogels lack severe eye-irritating effects. However, the use of alternative methods is still desirable no single assay being able to correctly predict the full spectrum of the UN GHS categories (Cat 1, serious, irreversible eye damage vs. Cat 2A, 2B reversible eye irritation) and thus, cannot fully replace the *in vivo* Draize eye irritation test (Lotz et al., 2016). Therefore, the combination of the BCOP assay with other internationally accepted test methods in a tiered testing strategy is suggested to allow the detailed and structured investigation of eye irritation potential that might be implemented in future (Kolle et al., 2016; Scott et al., 2010).

In summary, the observed interaction of the studied tNGs with primary keratinocytes and the HaCaT cell line and the interpretation of the consequences of the particle fate and behavior within the cells indicate the good biocompatibility for these polymeric nanocarriers.

## Conclusions

In the present study, we investigated the uptake and localization of tPG and pNIPAM-based dendritic nanogels as well as their toxicological potential in human keratinocytes. As clearly confirmed by laser scanning confocal microscopy, the nanogels were taken up by the cells and mainly localized within the lysosomes after 24 h of incubation. In addition to uptake studies, we determined the biocompatibility of tNGs in primary derived keratinocytes, the predominant cell type of the viable epidermis of human skin, by MTT assay, comet assay and Carboxy-H2DCFDA-assay. Additionally, eye irritation potential was determined by BCOP and RBC test. Both pNIPAM and tPG-based nanogels exhibited no adverse effects with regard to cytotoxicity, oxidative stress induction and genotoxicity. Moreover, both tested tNGs were devoid of eye irritation potential. Interestingly, the studied tNGs have a high-loading capacity of the lipophilic model drugs DX and TAC and are capable of releasing their payload into the viable part of the skin, before they are taken up by the non-targeted keratinocytes which highlights the tNGs as promising drug-delivery carrier. In summary, our studies underline the potential of tNGs as a dermal drug-delivery system for the treatment of skin diseases.

## Acknowledgements

We thank Guy Yealland for language editing and Monika Haseloff for the excellent technical assistance.

## Disclosure statement

The authors declare that this article content has no conflicts of interest.

## Funding

This work was financially supported by the German Research Foundation (Collaborative Research Center SFB1112, project A04:

M.C., M.G., project B02: M.M., S.L., project C02: S.H, G.Y., project Z01: M.S.-K., B.K., N.M., C.G., A.E., F.N., A.S., N.Z.).

## References

- Ahlberg S, Meinke MC, Werner L, Epple M, Diendorf J, Blume-Peytavi U, et al. 2014. Comparison of silver nanoparticles stored under air or argon with respect to the induction of intracellular free radicals and toxic effects toward keratinocytes. *Eur J Pharm Biopharm* 88:651–7.
- Asadian-Birjand M, Bergueiro J, Rancan F, Cuggino JC, Mutihac RC, Achazi K, et al. 2015. Engineering thermoresponsive polyether-based nanogels for temperature dependent skin penetration. *Polym Chem* 6:5827–31.
- Asadian-Birjand M, Sousa-Herves A, Steinhilber D, Cuggino JC, Calderon M. 2012a. Functional Nanogels for Biomedical Applications. *Curr Med Chem* 19:5029–43.
- Asadian-Birjand M, Sousa-Herves A, Steinhilber D, Cuggino JC, Calderon M. 2012b. Functional nanogels for biomedical applications. *Curr Med Chem* 19:5029–43.
- Bergueiro J, Calderon M. 2015. Thermoresponsive nanodevices in biomedical applications. *Macromol Biosci* 15:183–99.
- Contri RV, Fiel LA, Alnasif N, Pohlmann AR, Guterres SS, Schafer-Korting M. 2016. Skin penetration and dermal tolerability of acrylic nanocapsules: influence of the surface charge and a chitosan gel used as vehicle. *Int J Pharm* 507:12–20.
- Cooke MS, Evans MD, Dizdaroglu M, Lunec J. 2003. Oxidative DNA damage: mechanisms, mutation, and disease. *FASEB J* 17:1195–214.
- Cuggino JC, Alvarez CI, Strumia MC, Welker P, Licha K, Steinhilber D, et al. 2011a. Thermosensitive nanogels based on dendritic polyglycerol and N-isopropylacrylamide for biomedical applications. *Soft Matter* 7:11259–66.
- Cuggino JC, Strumia MC, Igarzabal CIA. 2011b. Synthesis, characterization and slow drug delivery of hydrogels based in N-acryloyl-tris-(hydroxymethyl) aminomethane and N-isopropyl acrylamide. *React Funct Polym* 71:440–6.
- Döge N, Hönzke S, Schumacher F, Balzus B, Colombo M, Hadam S, et al. 2016. Ethyl cellulose nanocarriers and nanocrystals differentially deliver dexamethasone into intact, tape-stripped or sodium lauryl sulfate-exposed *ex vivo* human skin – assessment by intradermal microdialysis and extraction from the different skin layers. *J Control Release* 242:25–34.
- Dommerholt J, Schmidt S, Temming R, Hendriks LJ, Rutjes FP, Van Hest JC, et al. 2010. Readily accessible bicyclononynes for biorthogonal labeling and three-dimensional imaging of living cells. *Angew Chem Int Ed Engl* 49:9422–5.
- Donaldson K, Stone V, Tran CL, Kreyling W, Borm PJ. 2004. Nanotoxicology. *Occup Environ Med* 61:727–8.
- Eom HJ, Choi J. 2010. p38 MAPK activation, DNA damage, cell cycle arrest and apoptosis as mechanisms of toxicity of silver nanoparticles in Jurkat T cells. *Environ Sci Technol* 44:8337–42.
- Fischer W, Calderon M, Schulz A, Andreou I, Weber M, Haag R. 2010. Dendritic polyglycerols with oligoamine shells show low toxicity and high siRNA transfection efficiency *in vitro*. *Bioconjug Chem* 21:1744–52.
- Gervais M, Brocas AL, Cendejas G, Deffieux A, Carlotti S. 2010. Synthesis of linear high molar mass glycidol-based polymers by monomer-activated anionic polymerization. *Macromolecules* 43:1778–84.

- Giulbudagian M, Asadian-Birjand M, Steinhilber D, Achazi K, Molina M, Calderon M. 2014. Fabrication of thermoresponsive nanogels by thermo-nanoprecipitation and in situ encapsulation of bioactives. *Polym Chem* 5:6909–13.
- Goyal R, Macri LK, Kaplan HM, Kohn J. 2016. Nanoparticles and nanofibers for topical drug delivery. *J Control Release* 240:77–92.
- Gysler A, Lange K, Korting HC, Schafer-Korting M. 1997. Prednicarbate biotransformation in human foreskin keratinocytes and fibroblasts. *Pharm Res* 14:793–7.
- Hackenberg S, Scherzed A, Kessler M, Hummel S, Technau A, Froelich K, et al. 2011. Silver nanoparticles: evaluation of DNA damage, toxicity and functional impairment in human mesenchymal stem cells. *Toxicol Lett* 201:27–33.
- Hofmann-Antenbrink M, Grainger DW, Hofmann H. 2015. Nanoparticles in medicine: Current challenges facing inorganic nanoparticle toxicity assessments and standardizations. *Nanomedicine* 11:1689–94.
- Hönzke S, Gerecke C, Elpelt A, Zhang N, Unbehauen M, Kral V, et al. 2016. Tailored dendritic core-multishell nanocarriers for efficient dermal drug delivery: a systematic top-down approach from synthesis to preclinical testing. *J Control Release* 242:50–63.
- Iversen TG, Skotland T, Sandvig K. 2011. Endocytosis and intracellular transport of nanoparticles: present knowledge and need for future studies. *Nano Today* 6:176–85.
- Kabanov AV, Vinogradov SV. 2009. Nanogels as pharmaceutical carriers: finite networks of infinite capabilities. *Angew Chem Int Ed* 48:5418–29.
- Kim DH, Martin DC. 2006. Sustained release of dexamethasone from hydrophilic matrices using PLGA nanoparticles for neural drug delivery. *Biomaterials* 27:3031–7.
- Kolle SN, Sauer UG, Moreno MC, Teubner W, Wohlleben W, Landsiedel R. 2016. Eye irritation testing of nanomaterials using the EpiOcular eye irritation test and the bovine corneal opacity and permeability assay. *Part Fibre Toxicol* 13:18.
- Koster RA, Alffenaar JW, Greijdanus B, Uges DR. 2013. Fast LC-MS/MS analysis of tacrolimus, sirolimus, everolimus and cyclosporin A in dried blood spots and the influence of the hematocrit and immunosuppressant concentration on recovery. *Talanta* 115:47–54.
- Kumar S, Alnasif N, Fleige E, Kurniasih I, Kral V, Haase A, et al. 2014. Impact of structural differences in hyperbranched polyglycerol-polyethylene glycol nanoparticles on dermal drug delivery and biocompatibility. *Eur J Pharm Biopharm* 88:625–34.
- Kumaravel TS, Vilhar B, Faux SP, Jha AN. 2009. Comet Assay measurements: a perspective. *Cell Biol Toxicol* 25:53–64.
- Lotz C, Schmid FF, Rossi A, Kurdyn S, Kampik D, De Wever B, et al. 2016. Alternative methods for the replacement of eye irritation testing. *Altex* 33:55–67.
- Mak WC, Patzelt A, Richter H, Renneberg R, Lai KK, Ruhl E, et al. 2012. Triggering of drug release of particles in hair follicles. *J Control Release* 160:509–14.
- Mukherjee SP, Byrne HJ. 2013. Polyamidoamine dendrimer nanoparticle cytotoxicity, oxidative stress, caspase activation and inflammatory response: experimental observation and numerical simulation. *Nanomedicine* 9:202–11.
- Naha PC, Bhattacharya K, Tenuta T, Dawson KA, Lynch I, Gracia A, et al. 2010. Intracellular localisation, geno- and cytotoxic response of polyN-isopropylacrylamide (PNIPAM) nanoparticles to human keratinocyte (HaCaT) and colon cells (SW 480). *Toxicol Lett* 198:134–43.
- Nel A, Xia T, Madler L, Li N. 2006. Toxic potential of materials at the nanolevel. *Science* 311:622–7.
- OECD. 2009. OECD, Test No. 437: Bovine corneal opacity and permeability test method for identifying i) chemicals inducing serious eye damage and ii) chemicals not requiring classification for eye irritation or serious eye damage. Paris, France: OECD Publishing.
- Pape PU. 1992. Red Blood Cell Test System Invitox Protocol No. 37 ERGATT/FRAME Databank of In Vitro Techniques in Toxicology.
- Petersen EJ, Nelson BC. 2010. Mechanisms and measurements of nanomaterial-induced oxidative damage to DNA. *Anal Bioanal Chem* 398:613–50.
- Rancan F, Asadian-Birjand M, Dogan S, Graf C, Cuellar L, Lommatzsch S, et al. 2016. Effects of thermoresponsivity and softness on skin penetration and cellular uptake of polyglycerol-based nanogels. *J Control Release* 228:159–69.
- Rancan F, Giulbudagian M, Jurisch J, Blume-Peytavi U, Calderon M, Vogt A. 2017. Drug delivery across intact and disrupted skin barrier: identification of cell populations interacting with penetrated thermoresponsive nanogels. *Eur J Pharm Biopharm*. [Epub ahead of print]. doi: <http://dx.doi.org/10.1016/j.ejpb.2016.11.017>.
- Sahle FF, Giulbudagian M, Bergueiro J, Lademann J, Calderon M. 2017. Dendritic polyglycerol and N-isopropylacrylamide based thermoresponsive nanogels as smart carriers for controlled delivery of drugs through the hair follicle. *Nanoscale* 9:172–82.
- Samah NA, Williams N, Heard CM. 2010. Nanogel particulates located within diffusion cell receptor phases following topical application demonstrates uptake into and migration across skin. *Int J Pharm* 401:72–8.
- Schindelin J, Arganda-Carreras I, Frise E, Kaynig V, Longair M, Pietzsch T, et al. 2012. Fiji: an open-source platform for biological-image analysis. *Nat Methods* 9:676–82.
- Scott L, Eskes C, Hoffmann S, Adriaens E, Alepee N, Bufo M, et al. 2010. A proposed eye irritation testing strategy to reduce and replace in vivo studies using Bottom-Up and Top-Down approaches. *Toxicol in Vitro* 24:1–9.
- Shi M, Kwon HS, Peng Z, Elder A, Yang H. 2012. Effects of surface chemistry on the generation of reactive oxygen species by copper nanoparticles. *ACS Nano* 6:2157–64.
- Sun C, Wang X, Zheng Z, Chen D, Shi F, Yu D, Wu H. 2015. A single dose of dexamethasone encapsulated in polyethylene glycol-coated polylactic acid nanoparticles attenuates cisplatin-induced hearing loss following round window membrane administration. *Int J Nanomedicine* 10:3567–79.
- Wang Z, Cuddigan JL, Gupta SK, Meenach SA. 2016. Nanocomposite microparticles (nCMp) for the delivery of tacrolimus in the treatment of pulmonary arterial hypertension. *Int J Pharm* 512:305–13.
- Warheit DB, Hoke RA, Finlay C, Donner EM, Reed KL, Sayes CM. 2007. Development of a base set of toxicity tests using ultrafine TiO<sub>2</sub> particles as a component of nanoparticle risk management. *Toxicol Lett* 171:99–110.
- Witting M, Molina M, Obst K, Plank R, Eckl KM, Hennies HC, et al. 2015. Thermosensitive dendritic polyglycerol-based nanogels for cutaneous delivery of biomacromolecules. *Nanomedicine* 11:1179–87.
- Xu W, Ling P, Zhang T. 2014. Toward immunosuppressive effects on liver transplantation in rat model: tacrolimus loaded poly(ethylene glycol)-poly(D,L-lactide) nanoparticle with longer survival time. *Int J Pharm* 460:173–80.

- Yang Y, Sunoqrot S, Stowell C, Ji J, Lee CW, Kim JW, et al. 2012. Effect of size, surface charge, and hydrophobicity of poly(amidoamine) dendrimers on their skin penetration. *Biomacromolecules* 13:2154–62.
- Zhang Z, Tsai PC, Ramezanli T, Michniak-Kohn BB. 2013. Polymeric nanoparticles-based topical delivery systems for the treatment of dermatological diseases. *Wiley Interdiscip Rev Nanomed Nanobiotechnol* 5:205–18.
- Zhao L, Zhou Y, Gao Y, Ma S, Zhang C, Li J, et al. 2015. Bovine serum albumin nanoparticles for delivery of tacrolimus to reduce its kidney uptake and functional nephrotoxicity. *Int J Pharm* 483:180–7.